Published in final edited form as:
Colloids Surf B Biointerfaces. 2014 October 1; 122: 126–133. doi:10.1016/j.colsurfb.2014.06.060.

Novel Anti-infective Activities of Chitosan Immobilized Titanium Surface with Enhanced Osteogenic Properties

Niranjan Ghimire[a], **Jie Luo**[b], **Ruogu Tang**[b], **Yuyu Sun**[b,*], and **Ying Deng**[a,*]

[a]Department of Biomedical Engineering, University of South Dakota, 4800 North Career, Avenue, Sioux Falls, South Dakota 57107, USA

[b]Department of Chemistry, The University of Massachusetts, One University Avenue, Lowell, MA 01854,USA

Abstract

We have covalently immobilized chitosan onto a titanium (Ti) surface to manage implant-related infection and poor osseointegration, two of the major complications of orthopedic implants. The Ti surface was first treated with sulfuric acid (SA) and then covalently grafted with chitosan. Surface roughness, contact angle and surface zeta potential of the samples were markedly increased by the sulfuric acid treatment and the subsequent chitosan immobilization. The chitosan-immobilized Ti (SA-CS-Ti) showed two novel antimicrobial roles: it a) prevented the invasion and internalization of bacteria into the osteoblast-like cells, and b) significantly increased the susceptibility of adherent bacteria to antibiotics. In addition, the sulfuric acid-treated Ti (SA-Ti) and SA-CS-Ti led to significantly increased ($P<0.05$) osteoblast-like cell attachment, enhanced cell proliferation, and better osteogenic differentiation and mineralization of osteoblast-like cells.

Keywords

chitosan immobilization; antibiotic-susceptibility; invasion; internalization; osteogenic differentiation

Introduction

Approximately 40.3 million adults in the US have certain orthopedic disorders, and implants are widely used to manage such conditions[1]. Titanium (Ti) is one of the most important orthopedic implant materials [2–4]. However, infections around the implants and poor osseointegration, which may lead to implant failure, are two major concerns of such implants [5, 6]. In severe cases, the implants have to be surgically removed out of the body with an extra course of antibiotic therapies and a lengthened hospital stay.

[*]**Corresponding Authors** Professor Ying Deng, Ph.D., Tel: (+ 1) 605-367-7775, Fax: (+ 1) 605-367-7836, Ying.Deng@usd.edu, Professor Yuyu Sun, PhD, Tel: 978-934-3637, Fax: 978-934-3013, yuyu_sun@uml.edu.

Infection is one of the most common causes of implant failure [4, 6, 7]. Although pre-and post-surgical antibiotic prophylaxes are used and utmost caution is taken during surgeries in general practice, bacterial infections continue to be a significant clinical challenge. Such infections significantly increase treatment cost, cause patient pain and suffering as well as take away productivity [8]. One of the major causes of implant-associated infections is related to microbial biofilms formed on implant surfaces because most of the current device materials are susceptible to bacterial adhesion and biofilm formation[9–11] . There is substantial evidence that bacteria in a biofilm undergo phenotypic change that makes them less sensitive to antibiotics. Bacteria living in a biofilm are up to 1000 times more resistant to antibiotics than their floating counterparts [9–12]. Current methods to control implant biofilms include reducing bacterial attachment [13] or killing the adherent bacteria [14]. However, both techniques have their own downsides. The techniques for lowering the number of attached bacteria cannot completely prevent biofilm formation, and can also reduce bone cell attachment, leading to poor osseointegration. Although the local delivery of antibiotics incorporated within the implants has been demonstrated to be able to kill the bacteria, high doses of such locally-delivered antibiotics can be toxic and can inhibit osteogenic activity [12].

Another cause of implant related infections, particularly long-term ones, is associated with bacterial invasion/internalization (i-bacteria) within surrounding osteoblasts. The i-bacteria are protected by the osteoblasts from antibiotics and the host immune system, making the treatment very difficult [5, 15, 16].The ability of i-bacteria to infect other healthy cells after being released out of the osteoblasts has already been demonstrated *in vitro* [16]. I-bacteria have also been traced in the osteoblasts of patients with implant-related osteomyelitis, confirming the involvement of i-bacteria in the onset and persistence of the disease [17]. Implant materials that can prevent bacterial invasion and internalization are not now available. Such implants that discourage the bacterial internalization of the bacteria definitely would limit the incidence of infected-implant associated osteomyelitis.

It has been reported that about 56% of the revision surgeries are due to aseptic loosening mainly caused by poor biocompatibility and osseointegration, leading to failure of bone ingrowth into the implant [12, 18]. Smooth Ti implants have been reported to be less desirable for bone fixation than roughened ones because a rough Ti surface has shown better osteogenic activities such as cell attachment, cell proliferation and calcium deposition, proving to be beneficial for osseointegration. As a result, there has been a growing focus on increasing the surface roughness of the Ti implant. Acid etching is one of the most popular techniques to increase roughness for better osseointegration [19–22].

Considerable efforts have been devoted to address these issues, but success is still limited [6, 23–26].Here we show that a combination of two surface modifying techniques, sulfuric acid treatment and chitosan immobilization, could simultaneously address both issues of implant-related infection and poor osseointegration. The resulting chitosan-immobilized surface completely prevented invasion of bacteria into the pre-attached osteoblast-like cells, significantly increased the antibiotic susceptibility of adherent bacteria, and greatly enhanced osteogenic activity, offering an innovative strategy that could significantly improve the long-term success of prosthetic implants.

Materials and Methods

Sample Preparation

Ti foil (purity: 99.7%; 0.25 mm in thickness), dopamine hydrochloride, glutaraldehyde (25%), and chitosan (75–85% deacetylated; viscosity: 20–300 cP, 1 wt. % in 1% acetic acid at 25 °C) were purchased from Sigma-Aldrich. The Ti foil was cut into a series of 1×1 cm^2, ultrasonically cleaned sequentially in acetone, absolute ethanol, and distilled water (10 min each), and then dried under vacuum. The resulting samples were referred to as UN-Ti. The Ti samples were treated in 48% H_2SO_4 solution at 60°C under constant stirring for 3 h, washed extensively with distilled water, and dried under vacuum. These samples were designated as SA-Ti. In the preparation of chitosan-containing Ti (SA-CS-Ti), the SA-Ti samples were treated in 5mg/mL dopamine hydrochloride in 10% 0.1M TRIS-HCL aqueous solution at room temperature for 12 h, followed by immersion in 3% glutaraldehyde at 4°C overnight [27]. Afterwards, the samples were immersed in 0.5% chitosan solution (in 1% acetic acid aqueous solution) at room temperature for 18 h, rinsed with distilled water, and dried under a vacuum[28].

Contact Angle Measurement

The contact angles of different samples were measured by contact angle goniometry (VCA Optima goniometer) using distilled water. Three samples from each group were used, and five readings of each specimen were recorded to calculate the average contact angle. The images were taken at around 10 s of droplet delivery.

Surface Zeta Potential

The surface zeta potentials of the samples were measured using a particle analyzer (Beckman coulter DV 730 Delsa Nano C) with a flat flow cell. All the samples were autoclaved before the measurement of the surface zeta potential.

Surface Profilometry

The surface roughness of the samples was measured by optical profilometry using a WYKO NT8000 profilometer. The scanning area for the profilometry was 480×640 μm^2. All the samples were autoclaved before the measurement of the surface roughness.

X-ray Photoelectron Spectroscopy (XPS) Analysis

The surface chemical composition of the samples was measured using a VG Escalab MK II XPS equipped with monochromatic Al Kα radiation source (hν = 1486.6 eV). The voltage and current were 15 kV and 10 mA, respectively. Survey spectra were collected with pass energy of 100 eV and the rate of 1 eV/step, while region scans were performed using pass energy of 50 eV and the rate of 0.1 eV/step. For different samples C1s, N1s, O1s and S2p region were scanned. Before measurement all samples were autoclaved. The calculated binding energies were referenced to the C1s neutral carbon peak at 284.97 eV.

Bacterial Culture

In the bacterial invasion/internalization and susceptibility assays, *S. aureus* (ATCC 6538) was cultured in tryptic soya broth overnight at 37°C. The number of bacteria was determined by plate spreading, and a standard curve was generated by measuring the absorbance at 600 nm.

Bacteria and Cell Staining for Confocal Microscopy Studies

Confocal imaging was carried out with slight modification as described elsewhere [29] . The fresh pellets of overnight-grown bacteria were washed with PBS and resuspended in a 3 ml buffer (0.2 M Na_2CO_3/ $NaHCO_3$- NaCl, pH 9.2). A concentration of 0.1 mg fluorescein isothiocyanate (FITC, Sigma Aldrich) per 10^6 bacteria per ml buffer was added and the mixtures were covered with aluminum foil and incubated in an ice bath for 30 min. Osteoblast-like cells were pre-seeded on different Ti surfaces for 2 h, and the FITC-labeled bacteria were seeded onto the same Ti samples for 2 h. The specimens were taken out, washed with assay medium (DMEM medium without antibiotics), fixed with 2.5% glutaraldehyde in PBS for 15 min, and washed with PBS. The cells were then permeabilized with 0.2% Triton-X 100 in PBS for 10 min. An aliquot of 80 μl of 100 nM rhodamine phalloidin (Cytoskeleton, Inc.) was added and the mixture was reacted for 30 min at ambient temperature in the dark to stain the cells. Finally, the Ti samples were visualized using a confocal imaging system (Nikon A1 TIRF).

Bacterial Invasion/Internalization Assay

Briefly, the SaOS-2 cells were attached on the Ti substrates, as described above. After washing with PBS, freshly prepared bacteria (10^4–10^5 bacteria/sample) were added onto substrates to infect the cells. After 2 h of contact, the substrates were washed three times with assay medium (DMEM medium without antibiotics). An aliquot of 100 μg/ml gentamicin was added to the substrates for 2 h to inactivate extracellular bacteria. To confirm this, an aliquot of the suspension thus obtained was plated onto agar plates to determine the colony forming units (CFUs). Cells on the substrates were lysed with 0.1% Triton-X 100 in PBS, and sonicated for 10 min to release the internalized and invaded bacteria. Finally, the level of bacteria released out of the lysed cells was quantified by agar plate spreading.

Antibiotic Sensitivity Assay for S. aureus

Antibiotic sensitivity assay for *S. aureus* was carried out following a published protocol with a slight change [29]. Briefly, 10^5 CFU/ml of bacterial suspension was added to each of the Ti substrates in a 24-well plate. After 2 h of incubation at 37 °C to allow bacterial attachment (the initial events of biofilm formation), the samples were taken out and washed with PBS. Then, 100 μg/ml of gentamicin was added to each sample. After 2 h of contact, the level of recoverable bacteria on the surface was determined by agar plate spreading.

SaOS-2 Cell Culture

Osteoblast-like cells, SaOS-2 (ATCC number: HTB-85), were cultured in DMEM (Fischer Scientific) medium supplemented with 10 % FBS, 1 % antibiotics (penicillin/streptomycin)

and 1% essential amino acid. The cells were grown in 75 cm^2 flasks under 37 °C in a humidified atmosphere of 95 % air and 5% CO_2. The growth medium was first changed after 24 h and then every 72 h. After the cells reached the confluence level of 80–90%, they were washed with PBS to remove the unattached cells and treated with trypsin. The cells were then centrifuged at 130 xg for 7 min. The supernatants were discarded and fresh culture medium was added to the pellets to make the desired concentration of the cells.

Cell Attachment Study

Osteoblast-like cell attachment assay was performed by following established protocol with slight modifications [13] . The Ti samples were placed on the 24-well plate and seeded with a density of 100,000 cells/ sample. The samples were incubated for 5 min, 120 min, 240 min and 480 min at 37°C and atmospheric condition of 5% CO_2 and 95% air. Then, the samples were washed with PBS to remove the unattached cells, and the number of attached cells was determined using MTT assay. For MTT assay, 200 μl of MTT (3-(4, 5-Dimethylthiazol-2-yl)-2, 5-diphenyltetrazolium bromide) solution (5mg/ml) was added to each of the Ti samples. After overnight incubation at ambient temperature under dark, the liquid was gently aspirated out of the sample solution without disturbing the crystals formed on the surface of the samples. The crystal was then dissolved in 500 μl of DMSO (dimethyl sulfoxide). 100 μl of the solution was placed in a 96-well plate and the absorbance at 570 nm was recorded using a microplate reader (TECAN Infinite M200). The cell number was calculated by normalizing absorbance value against a standard curve. The morphology and the density of the cells attached were observed using SEM.

Cell Proliferation Study

The proliferation of the cells on different samples was measured by counting the number of cells after 1, 3, 14, and 28 days of culture, following a slightly modified technique reported elsewhere [13]. Each sample in a 24-well plate was seeded with 10,000 cells and incubated at 37°C in an atmospheric condition of 95% air and 5% CO_2. At predetermined days, the samples were collected and rinsed with PBS to remove the unattached cells. Cell proliferation was determined using the MTT assay, as described above.

Mineralized Matrix Deposition Assay

The Ti samples were incubated in the cell growth medium supplemented with 50 μg/ml ascorbic acid and 10 mM sodium β-glycerophosphate [13] containing 100,000 cells. The amount of calcium deposited was measured after 28 and 42 days of culturing. After washing the samples with PBS, the samples were soaked with 500 μl of 0.5 M acetic acid to dissolve the calcium mineral deposited, and the content was determined using a calcium assay kit (DICA-500, Bioassay Systems, CA, USA). The mineralization on different samples at Day 28 was also observed using SEM.

ALP Activity Assay

Cells were seeded onto the samples at a density of 100,000 cells per cm^2 and the medium used was supplemented with 50 μg/ml ascorbic acid and 10 mM sodium glycerophosphate [13] . ALP assay was based on the hydrolysis of p-nitrophenyl phosphate into p-nitrophenol

at 37°C. ALP activity was determined after 7, 14 and 28 days of the cell seeding. The cells on the samples were washed with PBS and lysed with 0.2 % Triton X-100. The ALP was released out of the cells after sonicating for 10 min. The ALP assay was performed as described in the ALP kit manual (DALP-250, Bioassay Systems, CA, USA). Distilled water and tartrazine were used as negative control and positive control, respectively.

Statistical Analysis

For each bacterial and osteoblasts-like cell experiment, four samples per unit time were used. The results were expressed as mean ± standard deviation and were analyzed using student two-tailed paired t-tests. The difference observed was considered to be statistically significant when $p<0.05$.

Results

Surface modification and characterization

In this study, the Ti surface was treated with sulfuric acid before chitosan (75%-85% deacetylated) immobilization. The experimental/treated groups were sulfuric acid treated Ti (SA-Ti), the intermediate product, and chitosan immobilized Ti (SA-CS-Ti), the final product. Untreated Ti (UN-Ti) served as controls. Fig. 1 shows the optical profilometry images of the UN-Ti, SA-Ti and SA-CS-Ti surfaces. UN-Ti had a flat, smooth topography [Fig. 1a, Rz (maximum height) = 3.2 μm]. After the acid-chitosan modification, the surfaces appeared coarse with significantly increased height variation in SA-Ti (Fig. 1b, Rz = 11.25μm) and SA-CS-Ti (Fig. 1c, Rz = 7.91μm). The mean surface roughness value of UN-Ti was 0.190±0.007 μm, which was approximately tripled in SA-Ti (0.600 ± 0.153 μm) and SA-CS-Ti (0.700±0.053μm), as shown in Table 1.

Contact angle goniometry results showed that there was a significant increase in contact angle after the sulfuric acid treatment and the subsequent chitosan immobilization. Treated samples, SA-Ti and SA-CS-Ti, showed a significant increase ($P<0.05$) in the hydrophobicity with contact angles of 81.58°±9.16 and 94.10°±4.32, respectively, while the UN-Ti had a contact angle of 70.30°±0.68 (Table 1).

In order to determine if the surface modifications change surface charges, surface zeta potential was measured. UN-Ti had a negative zeta potential of −0.81±0.34 mV, and SA-Ti and SA-CS-Ti had positive surface zeta potentials of 5.56±0.51 mV and 4.14±0.16 mV, respectively (Table 1, $P<0.05$).

XPS analysis was used to determine surface chemical composition. While sulfur was not detected in UN-Ti, it was found on the surfaces of SA-Ti and SA-CS-Ti (Table 1, $P<0.05$).

Antimicrobial Property Evaluation

Prevention of the Bacteria Invasion/ Internalization—In the bacterial invasion tests, 10^5 osteoblast-like cells were pre-seeded on the sample surfaces, and the samples were then treated with 10^4–10^5 CFU (Colony Forming Unit)/ml of *S. aureus* for 2 h. In the confocal microscope study, i-bacteria (white circled) were observed in the osteoblast-like cells on UN-Ti (Fig. 2a) and SA-Ti (Fig. 2b), but not on SA-CS-Ti (Fig. 2c). To determine the exact

location of the same i-bacteria observed under the confocal microscope, three-dimensional (3D) views, x-y scans, and z-slices using the maximum intensity projection mode were presented, which confirmed the invasion/ internalization of the i-bacteria into the osteoblast-like cells on UN-Ti (Fig. 2d, g, white circled) and SA-Ti (Fig. 2e, h, white circled). In the case of SA-CS-Ti, however, bacteria either attached on the metal surfaces (Fig. 2f, thin white arrowed) or on the osteoblast-like cell surfaces (Fig. 2f, thick white arrowed); no invaded/internalized bacteria were observed.

As a further support for the confocal microscope results, although (260.00±34.76) and (316.70±76.37) CFU per sample of invaded or internalized bacteria could be isolated from UN-Ti and SA-Ti, no invaded or internalized bacteria could be recovered from SA-CS-Ti (Fig. 2j).

Increment in the Antibiotic-Sensitivity of Adherent Bacteria—To determine the antibiotic-susceptibility of the adherent bacteria, the bacteria were allowed to attach onto each testing surface (1×1 cm^2) for 2 h. We found that more than 3×10^3 CFU/cm^2 of bacteria adhered onto the surfaces of UN-Ti, SA-Ti and SA-CS-Ti; no significant differences were found between these three groups. The bacteria-containing samples were then soaked in broth solutions containing 100 μg/ml of gentamicin for 2 h. From UN-Ti and SA-Ti, 66.66±28.36 CFU and 150±50 CFU of adherent bacteria were recovered, respectively; however, no adherent bacteria could be recovered from the SA-CS-Ti (Fig. 2k), suggesting much higher antibiotic susceptibility.

Evaluation of Osteogenic Activities of Osteoblast-like Cells on Ti Surfaces

Cell Attachment Study—Cell attachment, one of the indicators of osteogenic activities of osteoblasts on implants, was evaluated using scanning electron microscopy (SEM). As shown in Fig. 3 a–r, on all the samples, the level of adherent cells gradually increased with the increase of contact time from 5 min (Fig. 3a,b,c), to 120 min (Fig. 3g,h,i) and then to 480 min (Fig.3m,n, o). At 120 min and 480 min, the cells attached on SA-Ti (Fig. 3k,q) and SA-CS-Ti (Fig. 3l,r) produced more extracellular matrix and became flattened earlier (suggesting faster spreading) than the cells attached on UN-Ti (Fig. 3j,p). Quantitative results in Fig. 3s further confirmed that a significantly higher ($P<0.05$) number of cells attached on the SA-Ti and SA-CS-Ti at 120 min and 240 min than on the UN-Ti. Moreover, after 480 min of seeding, although no significant difference could be observed on cell attachment density between SA-Ti and UN-Ti, significantly higher ($P<0.05$) number of cells attached onto SA-CS-Ti than on the surface of UN-Ti.

Cell Proliferation Study—Cell proliferation, another indicator of osteogenic activities of osteoblasts, was determined by calculating the number of cells proliferated on Days 1, 3, 14 and 28 (Fig.4). On Day 1, the number of cells on SA-Ti and SA-CS-Ti was significantly higher ($P<0.05$) than that on UN-Ti, suggesting an improved cell proliferation on SA-Ti and SA-CS-Ti. On Day 3, cell proliferation on SA-Ti was significantly higher ($P<0.05$) than on UN-Ti, and SA-CS-Ti showed a greater cell proliferation than UN-Ti. On Days 14 and 28, the trend of higher cell proliferation on SA-Ti and SA-CS-Ti than on UN-Ti continued,

confirming that the surfaced modification techniques we used led to a better cell proliferation.

Mineralized Matrices Deposition Assay—Mineralization is a widely used marker to evaluate osteoblast maturation. In the current study, SEM and calcium deposition tests were performed to determine the effect of the surface modifications on osteoblast mineralization. The 28-day SEM images (Fig. 5a, b, c) showed mineralized bead-like deposition (solid arrowed) on the surface of UN-Ti, SA-Ti and SA-CS-Ti, which suggested that cells on SA-Ti (Fig. 5b) and SA-CS-Ti (Fig. 5c) produced more mineral deposition than the cells on UN-Ti (Fig. 5a). In quantification studies (Fig. 5d), while the calcium deposition level on UN-Ti was significantly lower ($P<0.05$) on Day 28 than on Day 42, this level was not statistically different on SA-Ti and SA-CS-Ti on Days 28 and 42, suggesting faster calcium deposition on the modified Ti surfaces.

ALP Activity Assay—Osteoblast differentiation is one of the steps towards bone formation. Alkaline phosphatase (ALP) activity is a widely used marker for osteoblast differentiation. In this study, the time-dependent ALP activities of osteoblast-like cells on different samples after 7, 14 and 28 days of culture were shown in Fig. 5e. The ALP activity of the cells on SA-Ti and SA-CS-Ti was greater than that on UN-Ti throughout the experimental time period, and a significant difference ($P<0.05$) was found between UN-Ti (3.55±0.58) and SA-CS-Ti (18.96±8.10) on Day 14.

Discussion

In this study, we used acid etching followed by an immobilization of chitosan to modify the surface characteristics of Ti so as to achieve bacteria-resistant and osteogenic functions. It has been well established that UN-Ti surface contains various oxides which may include amorphous oxide, cubic titanium oxide (TiO), hexagonal titanium sesquioxide (Ti_2O_3), tetragonal titanium dioxide (TiO_2) (anatase), orthorhombic TiO_2 (brookite), tetragonal TiO_2 (rutile), and nonstoichiometric oxides (Ti_xO_y)[30]. These oxides attract H+, leaving OH- in the solution and generating a hydrophilic surface (low contact angle) with a weakly negative charge (Table 1). During sulfuric acid treatment, the strong acid reacted with the oxides to generate soluble products, and this etching led to a much rougher surface on SA-Ti. In our screening studies, we found that after 3 h of treatment, further increase in treatment time did not significantly change surface roughness of the resulting SA-Ti samples. The increase in contact angle after acid etching could be caused by the alternation in the crystalline structure of the surface oxides [30]. Moreover, SA-Ti showed a positive zeta potential (Table 1). Similar results were reported by other authors [31, 32], which could be due to the adsorption of the sulfate ions onto the surface and into the titanium hydride layer.

SA-CS-Ti was prepared through a three-step reaction. In the first step, SA-Ti was treated with dopamine overnight in the dark to introduce surface amino groups [27]. The discs were then treated with glutaraldehyde to introduce surface aldehyde groups. Finally, chitosan was used to treat the aldehyde-containing discs to produce SA-CS-Ti [28]. After these treatments, surface roughness of the resulting sample was not significantly affected as compared to that of SA-Ti (Table 1), indicating that chitosan chains were covalently

immobilized onto the SA-Ti surface, instead of forming layered physical coatings. The slight increase in contact angle of SA-CS-Ti could be caused by the hydrophobic alkyl chains of glutaraldehyde. As expected, SA-CS-Ti also showed a positive zeta potential (Table 1), which must be due to the presence of the amino groups on the chitosan.

UN-Ti, SA-Ti and SA-CS-Ti behaved significantly different in the bacteria-resistant assays. For one thing, although bacteria could readily invade SaOS-2 cells pre-attached on UN-Ti (Fig. 2a,d,g,j) and SA-Ti (Fig. 2d,e,h,j), no invaded/internalized bacteria could be found in SaOS-2 cells pre-attached on SA-CS-Ti (Fig. 2c,f,i,j). The mechanism for this effect is still not clear, but it is very likely related to the covalently bonded chitosan chains on SA-CS-Ti. It has been suggested that bacterial invasion to osteoblasts occurs via a receptor-mediated pathway, requiring the participation of cytoskeletal elements, principally actin [33, 34]. Since polycations like chitosan can bind actin and induce actin redistribution [35], it is possible that the chitosan-bonded surface inhibited receptor recycling, thereby preventing bacterial invasion of the SaOS-2 cells. This finding has significant clinical relevance. As noted earlier, there is growing evidence that bacteria, especially *Staphylococci*, can invade and be internalized by human osteoblasts [5, 15, 16]. The invaded osteoblasts then serve as internal bacteria reservoirs, causing recurrent diseases such as osteomyelitis and implant-related infections. The tissue surrounding an implant can thus act as a potential niche that protects bacteria from host defenses and antibiotic therapy. The new SA-CS-Ti effectively prevented the invasion of bacteria into osteoblast-like cells. This can be the first infection-control technology to prevent infections originating from bacteria residing in surrounding cells and tissues.

Furthermore, SA-CS-Ti surfaces significantly increased the antibiotic susceptibility of adherent bacteria (Fig. 2k). Bacterial adhesion and biofilm-formation on implant surfaces have serious consequences, including implant-related infection and device failure. Bacteria living in biofilms are far more resistant to antibiotic treatments than free-floating microorganisms [36, 37]. Effective antibiotic therapy therefore necessitates a high concentration of drugs in the tissue or space harboring the infectious microorganisms. However, high doses of systemically or locally delivered antibiotics can lead to toxicity and/or drug-resistance [38] . Here, we report that bacteria adherent on the new SA-CS-Ti were significantly more susceptible to antibiotics than bacteria on UN-Ti and SA-Ti, offering an innovative strategy for controlling bacterial adhesion and biofilm-related infections. This exciting new function can also be related to the covalently bonded chitosan chains on SA-CS-Ti. Even though the chitosan on the SA-CS-Ti was not able to completely disrupt the membrane of the bacteria on their surfaces, it might have increased the permeability of the bacterial membrane which eventually accelerated the sensitivity of the antibiotics towards bacteria. This is because the positively charged chitosan can bind to negatively charged bacteria membranes and chelate metal ions such as calcium and magnesium, both of which increase the permeability of bacterial cell walls [39], resulting in increased antibiotic susceptibility of the adherent bacteria.

SA-Ti and SA-CS-Ti showed very similar osteogenic functions. The acid treatment and the immobilization of chitosan onto the Ti surfaces enhanced the osteogenic/biologic activity of the osteoblast-like cells SaOS-2. SA-Ti and SA-CS-Ti sustained much higher initial cell

adhesion than UN-Ti (Fig 3), which could be mainly caused by the rougher surface of the former than that of the latter. A rough surface has been shown to form a direct contact with living bone[40] that might help in higher numbers of osteoblast-like cell attachment. This property is beneficial for osseointegration [41]. Another possibility can be related to surface charges. As cell surfaces are negatively charged, the positive charges on SA-Ti and SA-CS-Ti could act to attract more cells for attachment [42].

SA-Ti and SA-CS-Ti supported better cell proliferation than UN-Ti (Fig. 4). This result is consistent with the findings of previous studies [43, 44] . One of the possible mechanisms behind these might be related to modulation of the cytokines and growth factors of osteoblasts on rougher surfaces [44]. In addition, on SA-CS-Ti, the presence of chitosan chains could further enhance cell proliferation, which has been confirmed by previous reports [42, 45].

Cells on SA-Ti and SA-CS-Ti showed better ALP activity, a good indicator of osteoblastic differentiation and matrix mineralization. Again, these could be caused by the rough surface [19, 46, 47] as well as the positive charges [48] of the acid and chitosan modified samples. Better calcium deposition is desired for better osteoblast differentiation and osseointegration. That is the reason that, to improve the osseointegration, calcium phosphate coating is frequently used. However, such coating is brittle in nature and can fracture at the interface between the metals and the coating [49]. In our approach, the SA-CS-Ti does not have such concerns, which is particularly attractive for real applications.

Conclusions

Although chitosan is well known for its antimicrobial property, no previous report, to our knowledge, has described its role in 1) increasing antibiotic susceptibility of bacteria, and 2) limiting the invasion/internalization of bacteria into osteoblast. In this study, we reported these novel roles of chitosan surface treatments on Ti for controlling implant related infections. Furthermore, we demonstrated that chitosan surface treatments could improve the osteogenic property of implant materials. Thus, this work has provided a new insight in future implant design to simultaneously manage implant-related infection and poor osseointegration, two major clinical concerns of orthopedic implants.

Acknowledgments

We thank Ms. Kelly Graber from Sanford Research for providing the technical support required for the confocal microscopy. Research reported in this publication was supported by the National Institute of Arthritis and Musculoskeletal and Skin Diseases of the National Institutes of Health under Award Number R21AR065625. The content is solely the responsibility of the authors and does not necessarily represent the official views of the National Institutes of Health.

References

1. Statistics by Country for Orthopedic disorders. [(accessed 03/01/2013)] http://www.rightdiagnosis.com/o/orthopedic_disorders/stats-country.htm#extrapwarning
2. Geetha M, Singh AK, Asokamani R, Gogia AK. Ti based biomaterials, the ultimate choice for orthopaedic implants - A review. Progress in Materials Science. 2009; 54:397.

3. Degasne I, Basle MF, Demais V, Hure G, Lesourd M, Grolleau B, Mercier L, Chappard D. Effects of roughness, fibronectin and vitronectin on attachment, spreading, and proliferation of human osteoblast-like cells (Saos-2) on titanium surfaces. Calcif Tissue Int. 1999; 64:499. [PubMed: 10341022]
4. Bordji K, Jouzeau JY, Mainard D, Payan E, Netter P, Rie KT, Stucky T, Hage-Ali M. Cytocompatibility of Ti-6Al-4V and Ti-5Al-2.5Fe alloys according to three surface treatments, using human fibroblasts and osteoblasts. Biomaterials. 1996; 17:929. [PubMed: 8718939]
5. Montanaro L, Speziale P, Campoccia D, Ravaioli S, Cangini I, Pietrocola G, Giannini S, Arciola CR. Scenery of *Staphylococcus* implant infections in orthopedics. Future Microbiol. 2011; 6:1329. [PubMed: 22082292]
6. Kazemzadeh-Narbat M, Kindrachuk J, Duan K, Jenssen H, Hancock RE, Wang R. Antimicrobial peptides on calcium phosphate-coated titanium for the prevention of implant-associated infections. Biomaterials. 2010; 31:9519. [PubMed: 20970848]
7. Hetrick EM, Schoenfisch MH. Reducing implant-related infections: active release strategies. Chem Soc Rev. 2006; 35:780. [PubMed: 16936926]
8. Whitehouse JD, Friedman ND, Kirkland KB, Richardson WJ, Sexton DJ. The impact of surgical-site infections following orthopedic surgery at a community hospital and a university hospital: adverse quality of life, excess length of stay, and extra cost. Infect Control Hosp Epidemiol. 2002; 23:183. [PubMed: 12002232]
9. Costerton JW, Montanaro L, Arciola CR. Biofilm in implant infections: its production and regulation. The International journal of artificial organs. 2005; 28:1062. [PubMed: 16353112]
10. Hoiby N, Ciofu O, Johansen HK, Song ZJ, Moser C, Jensen PO, Molin S, Givskov M, Tolker-Nielsen T, Bjarnsholt T. The clinical impact of bacterial biofilms. Int J Oral Sci. 2011; 3:55. [PubMed: 21485309]
11. Arciola CR, Campoccia D, Gamberini S, Donati ME, Pirini V, Visai L, Speziale P, Montanaro L. Antibiotic resistance in exopolysaccharide-forming *Staphylococcus epidermidis* clinical isolates from orthopaedic implant infections. Biomaterials. 2005; 26:6530. [PubMed: 15949842]
12. Ratner, BDHA.; Schoen, FJ.; Lemons, JE. Biomaterials Science: An Introduction to Materials in Medicine. California, USA: Elsevier Academic Press San Diego; 2004.
13. Zhang F, Zhang Z, Zhu X, Kang ET, Neoh KG. Silk-functionalized titanium surfaces for enhancing osteoblast functions and reducing bacterial adhesion. Biomaterials. 2008; 29:4751. [PubMed: 18829101]
14. Jiang JL, Li YF, Fang TL, Zhou J, Li XL, Wang YC, Dong J. Vancomycin-loaded nano-hydroxyapatite pellets to treat MRSA-induced chronic osteomyelitis with bone defect in rabbits. Inflamm Res. 2012; 61:207. [PubMed: 22159524]
15. Hudson MC, Ramp WK, Nicholson NC, Williams AS, Nousiainen MT. Internalization of *Staphylococcus aureus* by cultured osteoblasts. Microb Pathog. 1995; 19:409. [PubMed: 8852281]
16. Ellington JK, Harris M, Webb L, Smith B, Smith T, Tan K, Hudson M. Intracellular *Staphylococcus aureus*. A mechanism for the indolence of osteomyelitis. J Bone Joint Surg Br. 2003; 85:918. [PubMed: 12931819]
17. Testoni F, Montanaro L, Poggi A, Visai L, Campoccia D, Arciola CR. Internalization by osteoblasts of two *Staphylococcus aureus* clinical isolates differing in their adhesin gene pattern. The International journal of artificial organs. 2011; 34:789. [PubMed: 22094558]
18. Kinov P, Leithner A, Radl R, Bodo K, Khoschsorur GA, Schauenstein K, Windhager R. Role of free radicals in aseptic loosening of hip arthroplasty. J Orthop Res. 2006; 24:55. [PubMed: 16419969]
19. Hott M, Noel B, Bernache-Assolant D, Rey C, Marie PJ. Proliferation and differentiation of human trabecular osteoblastic cells on hydroxyapatite. J Biomed Mater Res. 1997; 37:508. [PubMed: 9407299]
20. Ban S, Iwaya Y, Kono H, Sato H. Surface modification of titanium by etching in concentrated sulfuric acid. Dent Mater. 2006; 22:1115. [PubMed: 16375960]
21. Ban S, Taniki T, Sato H, Kono H, Iwaya Y, Miyamoto M. Acid etching of titanium for bonding with veneering composite resins. Dent Mater J. 2006; 25:382. [PubMed: 16916245]

22. de Souza Ferreira SB, de Assis Dias BR, Obregon CS, Gomes CC, de Araujo Pereira RR, Ribeiro Godoy JS, Estivalet Svidzinski TI, Bruschi ML. Microparticles containing propolis and metronidazole: in vitro characterization, release study and antimicrobial activity against periodontal pathogens. Pharmaceutical development and technology. 2014; 19:173. [PubMed: 23356908]
23. Norowski PA, Courtney HS, Babu J, Haggard WO, Bumgardner JD. Chitosan coatings deliver antimicrobials from titanium implants: a preliminary study. Implant Dent. 2011; 20:56. [PubMed: 21278528]
24. Giordano C, Sandrini E, Del Curto B, Signorelli E, Rondelli G, Di Silvio L. Titanium for osteointegration: Comparison between a novel biomimetic treatment and commercially exploited surfaces. J Appl Biomater Biomech. 2004; 2:35. [PubMed: 20803449]
25. Moursi AM, Winnard AV, Winnard PL, Lannutti JJ, Seghi RR. Enhanced osteoblast response to a polymethylmethacrylate-hydroxyapatite composite. Biomaterials. 2002; 23:133. [PubMed: 11762831]
26. Yazici H, Fong H, Wilson B, Oren EE, Amos FA, Zhang H, Evans JS, Snead ML, Sarikaya M, Tamerler C. Biological response on a titanium implant-grade surface functionalized with modular peptides. Acta Biomater. 2013; 9:5341. [PubMed: 23159566]
27. Fan X, Lin L, Dalsin JL, Messersmith PB. Biomimetic anchor for surface-initiated polymerization from metal substrates. J Am Chem Soc. 2005; 127:15843. [PubMed: 16277527]
28. Shi Z, Neoh KG, Kang ET, Poh C, Wang W. Bacterial adhesion and osteoblast function on titanium with surface-grafted chitosan and immobilized RGD peptide. J Biomed Mater Res A. 2008; 86:865. [PubMed: 18041731]
29. Amorena B, Gracia E, Monzon M, Leiva J, Oteiza C, Perez M, Alabart JL, Hernandez-Yago J. Antibiotic susceptibility assay for *Staphylococcus aureus* in biofilms developed in vitro. J Antimicrob Chemother. 1999; 44:43. [PubMed: 10459809]
30. Lim YJ, Oshida Y, Andres CJ, Barco MT. Surface characterizations of variously treated titanium materials. Int J Oral Maxillofac Implants. 2001; 16:333. [PubMed: 11432653]
31. Gold JM SM, Steinemann SG. XPS study of amino-acid adsorption to titanium surface. Helv. Phys. Acta. 1989; 62 246.
32. Brunette DM, TP.; Textor, M., et al. Titanium in Medicine Properties and biological significance of natural oxide films on titanium and its alloys. Springer; 2001. p. 171
33. Jevon M, Guo C, Ma B, Mordan N, Nair SP, Harris M, Henderson B, Bentley G, Meghji S. Mechanisms of internalization of *Staphylococcus aureus* by cultured human osteoblasts. Infect Immun. 1999; 67:2677. [PubMed: 10225942]
34. Zhang W, Ju J, Rigney T, Tribble G. Integrin alpha5beta1-fimbriae binding and actin rearrangement are essential for *Porphyromonas gingivalis* invasion of osteoblasts and subsequent activation of the JNK pathway. BMC Microbiol. 2013; 13:5. [PubMed: 23305098]
35. Amidi M, Mastrobattista E, Jiskoot W, Hennink WE. Chitosan-based delivery systems for protein therapeutics and antigens. Adv Drug Deliv Rev. 2010; 62:59. [PubMed: 19925837]
36. Raffa RB, Iannuzzo JR, Levine DR, Saeid KK, Schwartz RC, Sucic NT, Terleckyj OD, Young JM. Bacterial communication ("quorum sensing") via ligands and receptors: a novel pharmacologic target for the design of antibiotic drugs. J Pharmacol Exp Ther. 2005; 312:417. [PubMed: 15528454]
37. Parsek MR, Singh PK. Bacterial biofilms: an emerging link to disease pathogenesis. Annu Rev Microbiol. 2003; 57:677. [PubMed: 14527295]
38. Trampuz A, Zimmerli W. Antimicrobial agents in orthopaedic surgery: Prophylaxis and treatment. Drugs. 2006; 66:1089. [PubMed: 16789794]
39. Rabea EI, Badawy MET, Stevens CV, Smagghe G, Steurbaut W. Chitosan as antimicrobial agent: Applications and mode of action. Biomacromolecules. 2003; 4:1457. [PubMed: 14606868]
40. Hacking SA, Tanzer M, Harvey EJ, Krygier JJ, Bobyn JD. Relative contributions of chemistry and topography to the osseointegration of hydroxyapatite coatings. Clin Orthop Relat Res. 2002; 24
41. Boyan BD, Batzer R, Kieswetter K, Liu Y, Cochran DL, Szmuckler-Moncler S, Dean DD, Schwartz Z. Titanium surface roughness alters responsiveness of MG63 osteoblast-like cells to 1 alpha,25-(OH)2D3. J Biomed Mater Res. 1998; 39:77. [PubMed: 9429099]

42. Sheng-Wen Hsiao DVHT, Ho Ming-Hua, Hsieh Hsyue-Jen, Li Chung-Hsing, Hung Chang-Hsiang, Li Hsi-Hsin. Interactions between chitosan and cells measured by AFM. Biomedical Materials. 2010; 5:8.
43. Nishimura N, Kawai T. Effect of microstructure of titanium surface on the behaviour of osteogenic cell line MC3T3-E1. J Mater Sci Mater Med. 1998; 9:99. [PubMed: 15348915]
44. Kieswetter K, Schwartz Z, Hummert TW, Cochran DL, Simpson J, Dean DD, Boyan BD. Surface roughness modulates the local production of growth factors and cytokines by osteoblast-like MG-63 cells. J Biomed Mater Res. 1996; 32:55. [PubMed: 8864873]
45. Cai K, Frant M, Bossert J, Hildebrand G, Liefeith K, Jandt KD. Surface functionalized titanium thin films: zeta-potential, protein adsorption and cell proliferation. Colloids Surf B Biointerfaces. 2006; 50:1. [PubMed: 16679008]
46. Li LH, Kong YM, Kim HW, Kim YW, Kim HE, Heo SJ, Koak JY. Improved biological performance of Ti implants due to surface modification by micro-arc oxidation. Biomaterials. 2004; 25:2867. [PubMed: 14962565]
47. Schwartz Z, Lohmann CH, Oefinger J, Bonewald LF, Dean DD, Boyan BD. Implant surface characteristics modulate differentiation behavior of cells in the osteoblastic lineage. Adv Dent Res. 1999; 13:38. [PubMed: 11276745]
48. Hamamoto N, Hamamoto Y, Nakajima T, Ozawa H. Histological, histocytochemical and ultrastructural study on the effects of surface charge on bone formation in the rabbit mandible. Arch Oral Biol. 1995; 40:97. [PubMed: 7540834]
49. Johnson MHS, Narayan RJ, Snyder RL. In situ annealing of hydroxyapatite thin films. Materials Science and Engineering C. 2006; 26:1312.

Highlights

- Titanium surface was modified with chitosan and different properties were studied.
- The modification significantly increased antibiotic susceptibility of bacteria.
- The modification entirely prevented bacterial invasion into osteoblast-like cells.
- Osteogenic properties were noticeably improved with the chitosan modification.

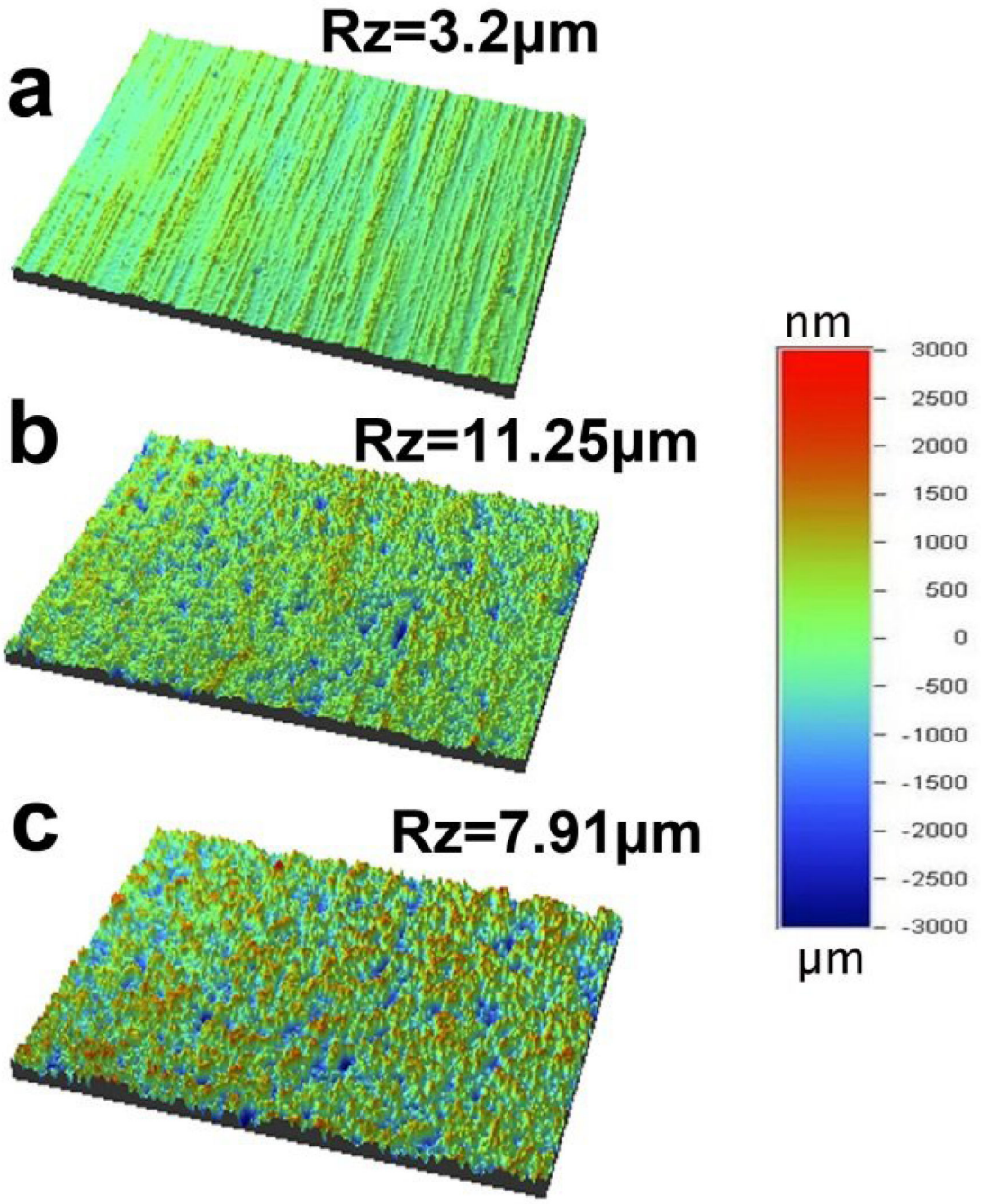

Figure 1.
Optical profilometry images of (a) UN-Ti, (b) SA-Ti, and (c) SA-CS-Ti.

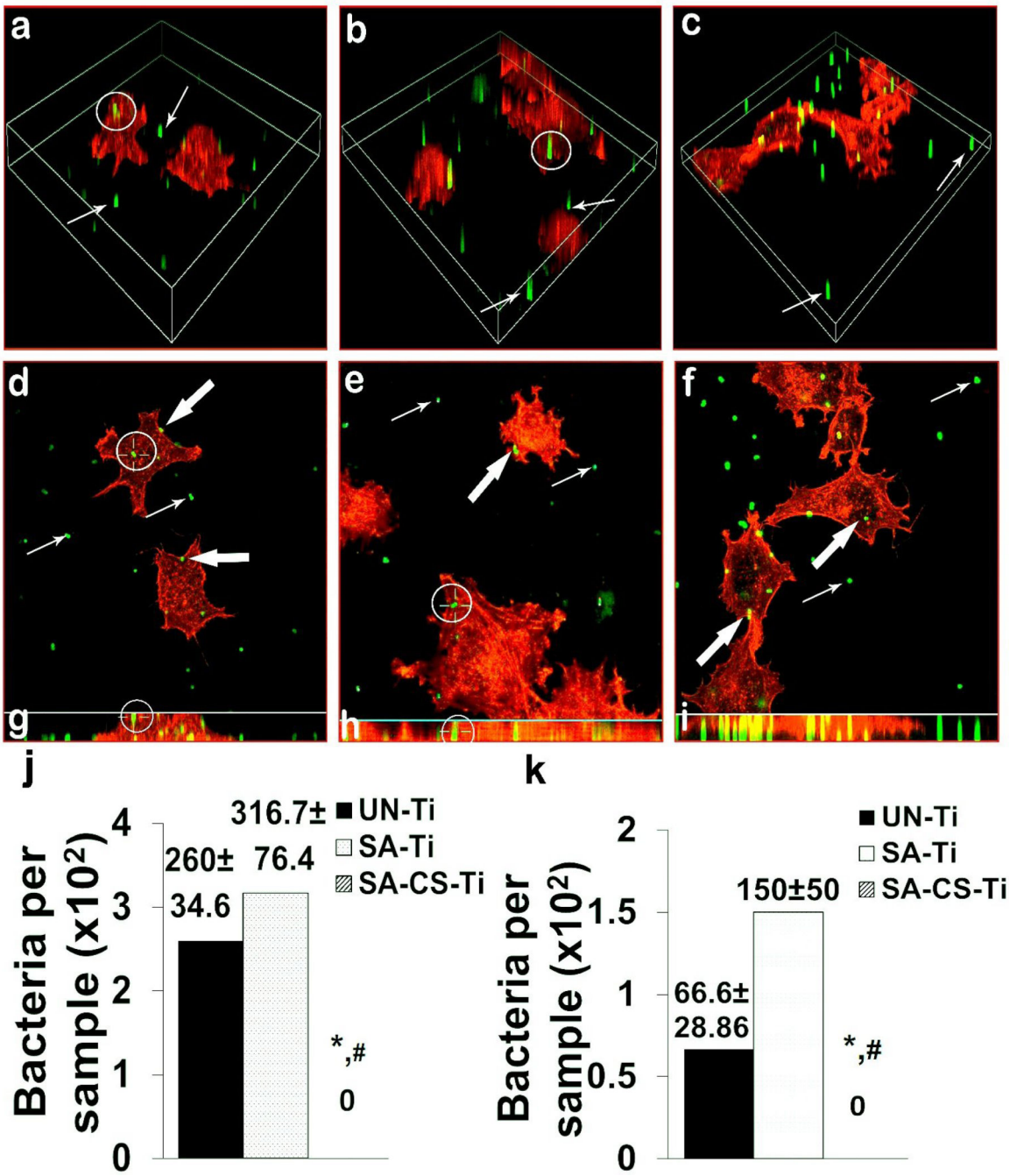

Figure 2.

Antimicrobial activity study. (a–c) Confocal microscopy 3D view was used to observe representative internalized bacteria (i-bacteria, white circled) on UN-Ti (a), SA-Ti (b) and SA-CS-Ti (c). (d–f) X–Y sections of representative images that showed the intracellular position of the same i-bacteria (white circled) on UN-Ti (d), SA-Ti (e) and SA-CS-Ti (f). (g–i) Vertical views obtained by combining the series of X–Y scans taken along the Z-axis at maximum intensity projection mode to show the intracellular position of the same i-bacteria (white circled) on UN-Ti (g), SA-Ti (h) and SA-CS-Ti (i). (j) Quantification of

internalized/invaded bacteria into the osteoblasts like cells on different materials (n=4). (k) Antibiotic susceptibility of bacteria on different samples (n=4). (*) denotes a significant difference ($p<0.05$) between the number of bacteria internalized on UN-Ti and SA-CS-Ti and (#) denotes significant difference ($P<0.05$) between UN-Ti and SA-CS-Ti.

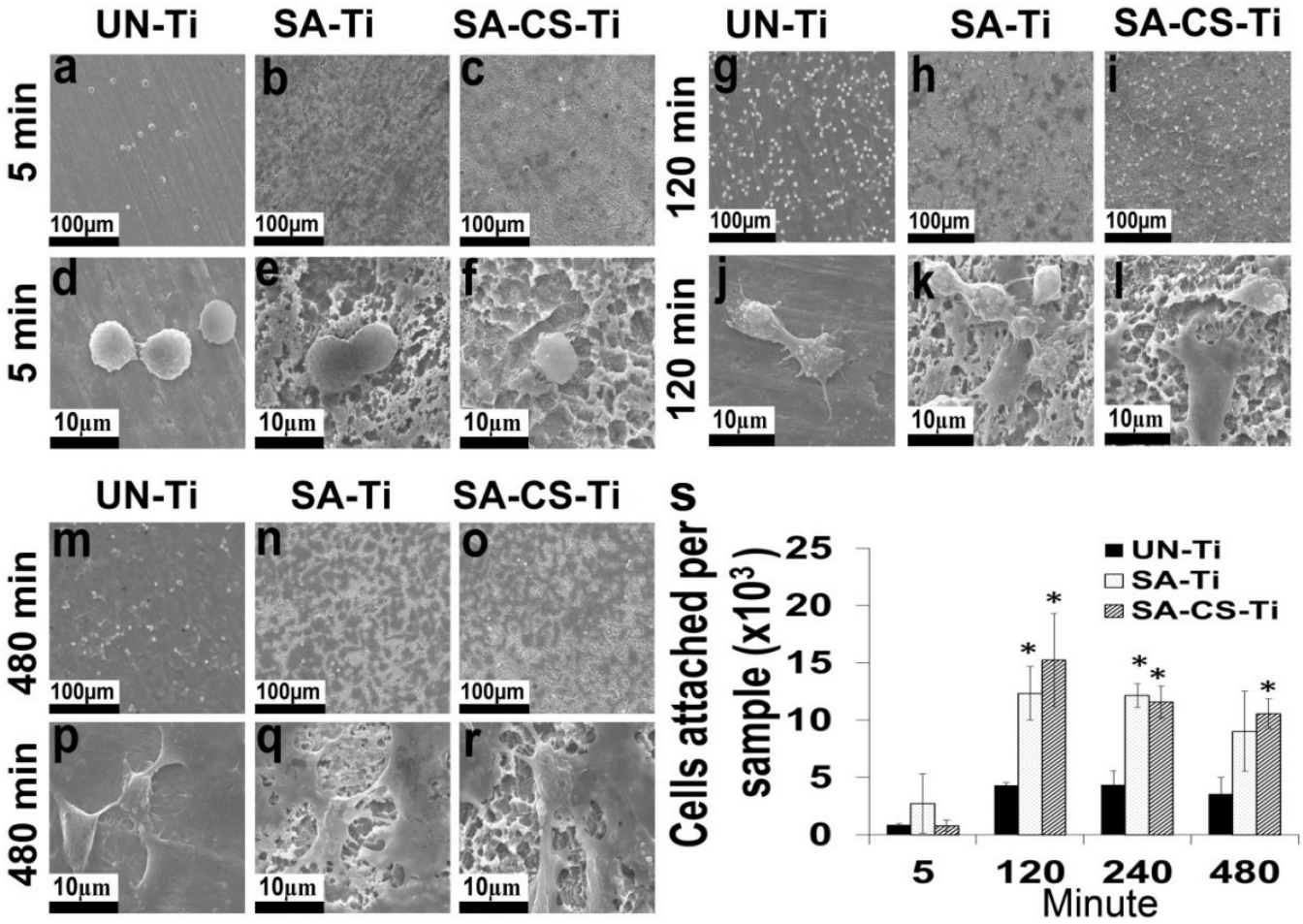

Figure 3.

Cell attachment study. (a–r) SEM micrographs of cells attached on UN- Ti, SA-Ti and SA-CS-Ti at 5 min (a–f), 120 min (g–l) and 480 min(m–r). (s) Quantitative comparison of osteoblast-like cell attachment at different time points. (*) denotes significant difference ($p<0.05$) compared with untreated titanium at respective time points.

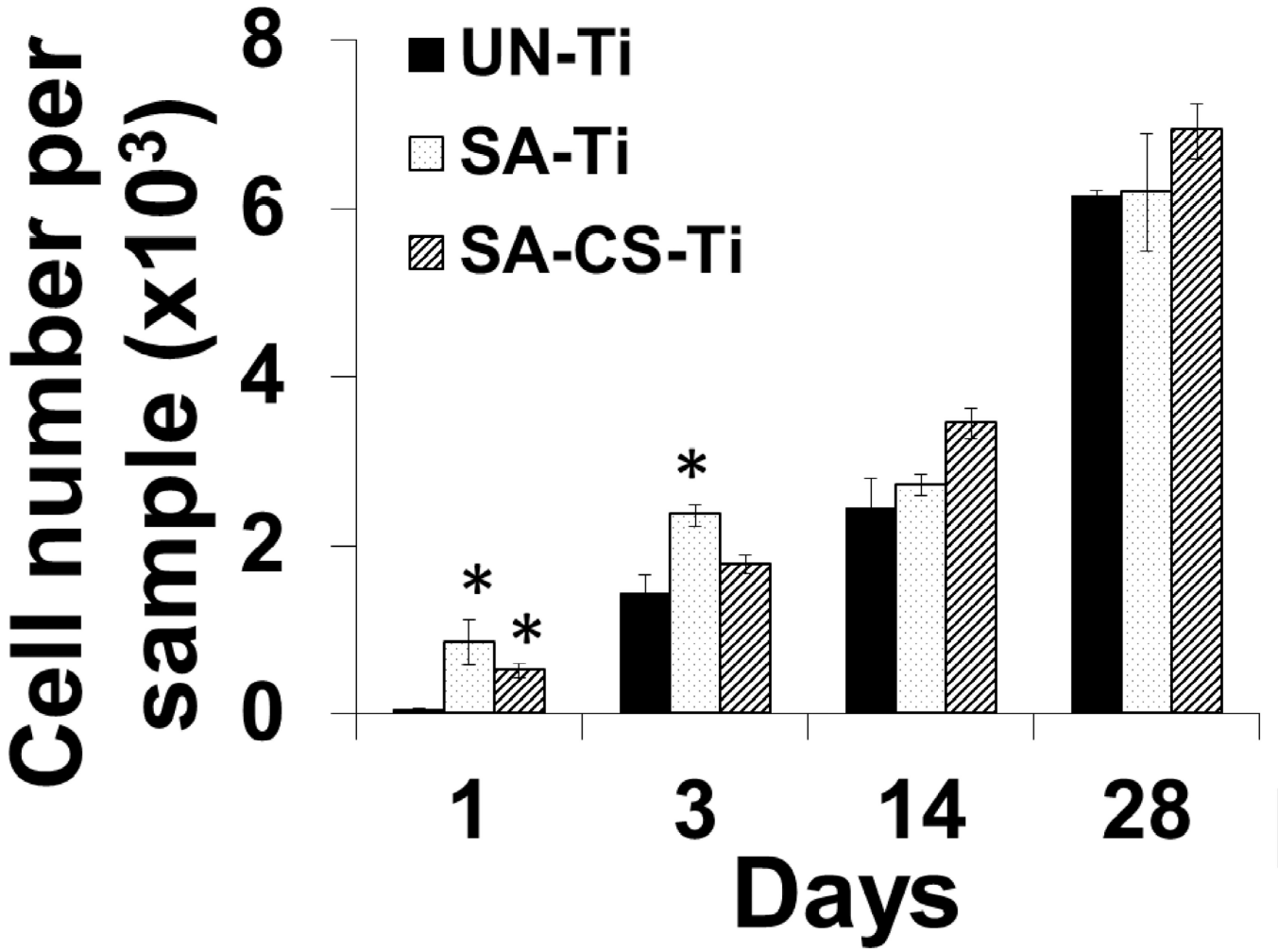

Figure 4.

Cell proliferation study. Osteoblast-like cell proliferation on UN-Ti, SA-Ti, and SA-CS-Ti surfaces after 1,3,14 and 28 days of culture. (*) denotes significant difference ($p<0.05$) compared with untreated titanium at respective time points.

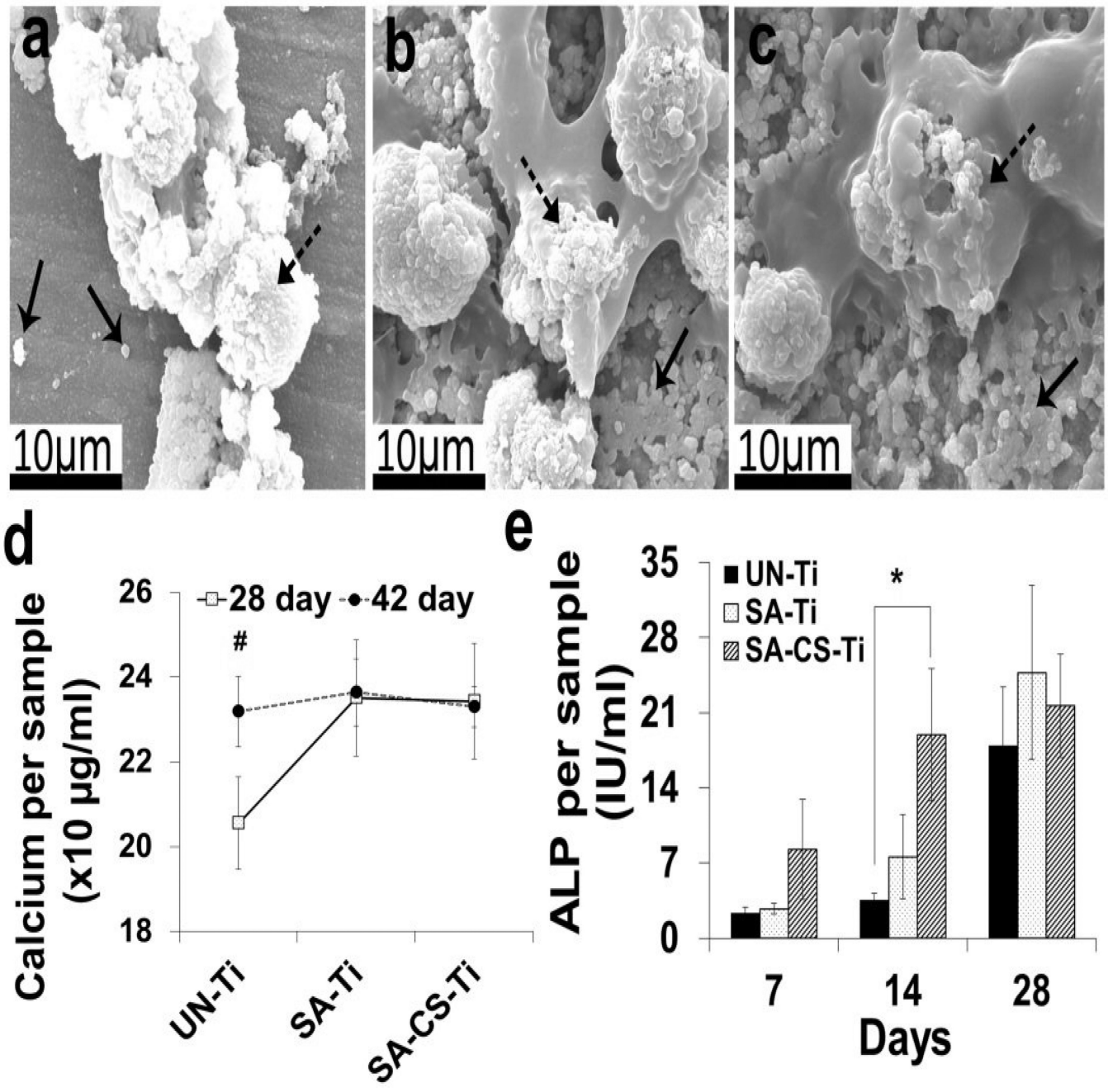

Figure 5.

Cell maturation and differentiation study. (a–c) SEM images of mineralized matrix deposition on UN-Ti (a), SA-Ti (b) and SA-CS-Ti (c) on Day 28. Solid arrows show the mineralized matrices deposited on the sample surfaces and dashed arrows show cells on the sample surfaces. (d) Quantitative representation of calcium deposition on UN-Ti, SA-Ti and SA-CS-Ti on Days 28 and 42 (n=4). (#) denotes significant increase in the calcium deposition ($p<0.05$) from Day 28 to Day 42 within the same experimental groups. (e)ALP

activity on UN-Ti, SA-Ti and SA-CS-Ti on Days 7, 14 and 28 (n=4). (*) denotes significant difference ($p<0.05$) compared with untreated titanium at respective time points.

Table 1

Surface characterization of UN-Ti, SA-Ti and SA-CS-Ti. Rz is the maximum height of the micro-pits formed. Surface nitrogen and sulfur contents were calculated from XPS data.

	UN-Ti	SA-Ti	SA-CS-Ti
Average roughness(μm)	0.190±0.007	0.600±0.153*	0.700±0.053*
Contact Angle (°)	70.30±0.68	81.58±9.16*	94.10±4.32*
Surface Zeta Potential (mV)	−0.81±0.34	5.56±0.51*	4.15±1.01*
Surface nitrogen content (%)	2.28 ± 0.48	1.48 ± 0.29	6.08 ± 0.16*
Surface sulfur content (%)	***ND***	0.24 ± 0.02*	0.22 ± 0.02*

(*) denotes significant difference ($p<0.05$) compared with untreated titanium. ND represents no detection.